

University of Nebraska - Lincoln

DigitalCommons@University of Nebraska - Lincoln

Biochemistry -- Faculty Publications

Biochemistry, Department of

6-1-2022

Altered collective mitochondrial dynamics in the Arabidopsis *msh1* mutant compromising organelle DNA maintenance

Joanna M. Chustecki

Ross D. Etherington

Daniel J. Gibbs

Iain G. Johnston

Follow this and additional works at: <https://digitalcommons.unl.edu/biochemfacpub>




Part of the [Biochemistry Commons](#), [Biotechnology Commons](#), and the [Other Biochemistry, Biophysics, and Structural Biology Commons](#)

This Article is brought to you for free and open access by the Biochemistry, Department of at DigitalCommons@University of Nebraska - Lincoln. It has been accepted for inclusion in Biochemistry -- Faculty Publications by an authorized administrator of DigitalCommons@University of Nebraska - Lincoln.

RESEARCH PAPER

Altered collective mitochondrial dynamics in the *Arabidopsis msh1* mutant compromising organelle DNA maintenance

Joanna M. Chustecki¹, Ross D. Etherington¹, Daniel J. Gibbs¹ and Iain G. Johnston^{2,3,*} 

¹ School of Biosciences, University of Birmingham, Birmingham B15 2TT, UK

² Department of Mathematics, University of Bergen, Realfagbygget, Bergen 5007, Norway

³ Computational Biology Unit, University of Bergen, Høyteknologisenteret i Bergen, Bergen 5008, Norway

* Correspondence: iain.johnston@uib.no

Received 20 April 2022; Editorial decision 30 May 2022; Accepted 1 June 2022

Editor: Toshihiro Obata, University of Nebraska-Lincoln, USA

Abstract

Mitochondria form highly dynamic populations in the cells of plants (and almost all eukaryotes). The characteristics and benefits of this collective behaviour, and how it is influenced by nuclear features, remain to be fully elucidated. Here, we use a recently developed quantitative approach to reveal and analyse the physical and collective ‘social’ dynamics of mitochondria in an *Arabidopsis msh1* mutant where the organelle DNA maintenance machinery is compromised. We use a newly created line combining the *msh1* mutant with mitochondrially targeted green fluorescent protein (GFP), and characterize mitochondrial dynamics with a combination of single-cell time-lapse microscopy, computational tracking, and network analysis. The collective physical behaviour of *msh1* mitochondria is altered from that of the wild type in several ways: mitochondria become less evenly spread, and networks of inter-mitochondrial encounters become more connected, with greater potential efficiency for inter-organelle exchange—reflecting a potential compensatory mechanism for the genetic challenge to the mitochondrial DNA population, supporting more inter-organelle exchange. We find that these changes are similar to those observed in *friendly*, where mitochondrial dynamics are altered by a physical perturbation, suggesting that this shift to higher connectivity may reflect a general response to mitochondrial challenges, where physical dynamics of mitochondria may be altered to control the genetic structure of the mtDNA population.

Keywords: *Arabidopsis thaliana*, mitochondrial dynamics, *msh1*, social networks, time-lapse microscopy.

Introduction

Mitochondria are key bioenergetic compartments of the eukaryotic cell. Within plant cells, hundreds of mitochondria exist, largely as individual organelles—contrasting with the reticulated network form often seen in yeast and mammalian cells (Logan, 2006b; Johnston, 2019). These cellular populations are highly dynamic (Logan, 2010), interacting with each other and with other organelles (Islam *et al.*, 2009; Jaipargas *et al.*,

2015; Shai *et al.*, 2016; Barton *et al.*, 2018; Krupinska *et al.*, 2020; Chustecki *et al.*, 2021).

Housed within these organelles, mitochondrial DNA (mtDNA) encodes essential information for the mitochondrial machinery. In plant cells, again contrasting with other kingdoms, different mitochondria contain different subsets of the full mtDNA genome (Preuten *et al.*, 2010). Many mitochondria

may contain no mtDNA at all, while some may contain the full genome (57 genes across 366 kb in *Arabidopsis*), and others may contain a subgenomic molecule containing some but not all mtDNA genes (Arimura *et al.*, 2004; Gualberto *et al.*, 2014; Kozik *et al.*, 2019). Processes of mtDNA exchange and recombination are essential to maintain this diverse structure (Bellaoui *et al.*, 1998; Arrieta-Montiel *et al.*, 2009; Davila *et al.*, 2011; Gualberto and Newton, 2017), with mtDNA sharing through the population of mitochondria constituting a ‘discontinuous whole’ (Logan, 2006a).

Such sharing and recombination is inherently shaped and limited by the physical behaviour of organelles in the cell (Belliard *et al.*, 1979; Lonsdale *et al.*, 1988; Gualberto and Newton, 2017; Aryaman *et al.*, 2019; Johnston, 2019; Rose, 2021). In order for this sharing to occur, mitochondria must physically meet and exchange contents—so the genetic structure of the mtDNA population is inherently controlled by the physical dynamics of the mitochondrial compartments.

Recent work suggested that the collective cellular dynamics of plant mitochondria can resolve a tension between mitochondrial proximity and spacing (Chustecki *et al.*, 2021). Mitochondria need to be physically proximal to allow membrane fusion and mixing of contents including mtDNA (Arimura *et al.*, 2004; Sheahan *et al.*, 2005; Rose, 2021). In addition to this exchange, mitochondrial proximity facilitates metabolic exchange and mitochondrial quality control, a process reliant on cycles of fission and fusion, key for maintaining a healthy chondriome (Jones, 1986; Karbowski and Youle, 2003; Arimura *et al.*, 2004; Logan, 2006a; Takanashi *et al.*, 2006; Twig *et al.*, 2008; Liu *et al.*, 2009; Figge *et al.*, 2012; Shutt and McBride, 2013; Agrawal *et al.*, 2018). There are also many other functional implications of inter-mitochondrial proximity including an influence on membrane potential (Santo-Domingo *et al.*, 2013), cristae alignment (Picard *et al.*, 2015), and calcium waves (Ichas *et al.*, 1997). However, there are also benefits to mitochondria remaining physically spaced, including for energy demand, inter-organelle co-localization, and the regulation of metabolic demands (Chen and Chan, 2006; Seguí-Simarro and Staehelin, 2009; Bauwe *et al.*, 2010; Sage *et al.*, 2012; Liesa and Shirihai, 2013; Spillane *et al.*, 2013; Shai *et al.*, 2016; Yu *et al.*, 2016; Schuler *et al.*, 2017; Yu and Pekkurnaz, 2018). The mitochondrial population thus faces a tension between maintaining even spacing of mitochondria and supporting inter-mitochondrial encounters.

Chustecki *et al.* (2021) explored this trade-off between even spacing and supporting encounters by characterizing the ‘social networks’ of the dynamic cellular population, allowing the analysis of connectivity across the chondriome—the whole population of mitochondria in a cell (Logan, 2010). Physical and network analysis revealed that wild-type *Arabidopsis* uses mitochondrial dynamics to resolve this tension, with mitochondrial motion allowing transient encounters between organelles—and facilitating efficient exchange through the population—while also retaining physical spacing. The

development of this approach allows targeted, quantitative questions to be asked about how collective mitochondrial behaviour responds to different situations. In particular, the question of whether and how the cell may control this behaviour in the face of genetic challenges to the mtDNA population remains open (Johnston, 2019). That is, if mtDNA integrity is compromised, can the cell compensate—at least in part—through adapting its control of mitochondrial dynamics?

Here, we pursue this question by investigating the collective behaviour of mitochondria in the *msh1* mutant. Here, MutS HOMOLOGUE 1 (MSH1), responsible for recombination surveillance and repair of organellar genomes (Martínez-Zapater *et al.*, 1992; Abdelnoor *et al.*, 2003, 2006; Shedge *et al.*, 2007; Arrieta-Montiel *et al.*, 2009; Davila *et al.*, 2011; Wu *et al.*, 2020) and the rapid segregation of mtDNA heteroplasmy (Broz *et al.*, 2022), is compromised. Disruption of mitochondrial-localized MSH1 leads to an increase in single nucleotide variants and insertion–deletion mutations in mtDNA (Wu *et al.*, 2020), and MSH1 disruption can also lead to stoichiometric shifting in the mitochondrial genome (Martínez-Zapater *et al.*, 1992; Sakamoto *et al.*, 1996; Abdelnoor *et al.*, 2003) [although the full molecular mechanism of MSH1 action on the mitochondrial genome is still not fully characterized (Fukui *et al.*, 2018; Wu *et al.*, 2020), multiple studies support the model of MSH1 influencing double-strand break repair (Davila *et al.*, 2011; Christensen, 2014; Wu *et al.*, 2020)]. *msh1* does not exclusively affect mtDNA: chloroplast maintenance is also compromised (Wu *et al.*, 2020), and downstream metabolic influences of the resulting organelle dysfunction also contribute to the phenotype (Xu *et al.*, 2011, 2012; Viridi *et al.*, 2015; Shao *et al.*, 2017).

Disruption of MSH1 thus provides genetic challenges to the mtDNA and plastid DNA (ptDNA) populations (as well as resultant metabolic and other stresses). We set out to investigate whether these challenges had the effect of changing the collective cellular behaviour of mitochondria. Following the above, we hypothesized that the plant cell might respond physically to compromised mtDNA maintenance, specifically by sacrificing spacing to facilitate more encounters and thus more exchange of mtDNA, and other mitochondrial contents, to compensate for the loss of genetic integrity and accompanying metabolic challenges. As described below, we explored this question by using single-cell microscopy, computational analysis, and network science approaches to characterize and analyse mitochondrial behaviour in *msh1* compared with wild-type *Arabidopsis* and other mutants.

Materials and methods

Plant lines

An MSH1 (previously CHM1-1) ethyl methanesulfonate-derived mutant line in the Columbia background generated by G. Redei (Rédei, 1973) was obtained from the *Arabidopsis* stock centre (N3372, http://arabidopsis.info/StockInfo?NASC_id=3372). This line carries a single nucleotide polymorphism (SNP) in the fourth exon of genomic region AT3G24320, leading to a non-synonymous glutamate→stop

codon change. This line was originally isolated in a *gl1* marked plant, a linkage gene in the third chromosome, and so carries a *gl1* polymorphism, and lacks trichomes. There is evidence to suggest that *gl1* does not alter mitochondrial behaviour (Islam *et al.*, 2020), and the gene is highly expressed in only the early shoot apical meristem (SAM), young leaf, and young flower, not in the hypocotyl used in this study (Nakabayashi *et al.*, 2005; Schmid *et al.*, 2005; Klepikova *et al.*, 2016). This mutant has been used in previous studies as a disruptor of normal MSH1 function (Xu *et al.*, 2011; Wu *et al.*, 2020). Seeds of *Arabidopsis thaliana* with mitochondrial matrix-targeted green fluorescent protein (GFP), and the mtGFP-*friendly* (Mito-GFP::*fmt*) line were kindly provided by Professor David Logan (Logan and Leaver, 2000; El Zawily *et al.*, 2014).

Crossing and DNA extraction

msh1 and mtGFP seeds were surface sterilized in 50% (v/v) household bleach solution for 4 min with continual inversion, rinsed three times with sterile water, and plated onto half-strength Murashige and Skoog (1/2 MS) agar. Plated seeds were stratified in the dark for 2 d at 4 °C. Seedlings were grown in 16 h light/8 h dark at 21 °C for 4–5 d, before being transferred to 4:2:1 compost-vermiculite-perlite mixture, and grown until the first flower buds developed. For day/night experiments, seedlings were grown at 22 °C in growth cabinets at 16 h light/8 h dark set to be mid-way (8 h) through the light period or mid-way through the dark period (4 h) at the point of imaging.

The crossing technique followed the protocol of Browse *et al.* (1993), with mtGFP plants as the pollen donor and *msh1* plants accepting. Pollinated stigmas were wrapped gently in plastic wrap, and siliques were left to develop. F₂ seeds were sown onto 50 µg ml⁻¹ kanamycin 1/2 MS (Murashige and Skoog) plates, selecting for individuals carrying the fluorescence construct (Logan and Leaver, 2000), and grown on soil as before. Leaf samples were taken for DNA extraction from all except F₂ seeds.

Quick DNA extraction was performed on young leaf samples (2–3 weeks old, age dependent on growth rate). Leaf samples were macerated with a pipette tip in 40 µl Extraction Buffer (2.5 ml of 2 M Tris-HCl, 500 µl of 1 M EDTA, 6.25 ml of 2 M KCl, made up to 50 ml with BPC water). The sample was then incubated in a heat block for 10 min at 95 °C. A 40 µl aliquot of dilution buffer was added [3% BSA (1.5 g in 50 ml), filter sterilized], and samples were spun down at 13 000 rpm for 60 s before storing at -20 °C.

Genotyping and sequencing

For genotyping, primer set 1 was used. A reverse primer (RP1, 5'AAAC TTCGCGTGAAACCTTGACTTAATGT 3') running into the SNP site was designed using dCAPS finder 2.0 (Neff *et al.*, 1998), and the forward primer (FP1, 5'CATCTCACCTTCTAGATGTCAGCCTTT 3') was designed 200 bp upstream of the restriction site. By design, *Bsr*GI will cut a region of 30 bp from the 293 bp element if the SNP is present, producing one larger (260 bp) and one smaller (~30 bp) fragment compared with the wild-type single fragment (293 bp). After PCR amplification, half (5 µl) of the PCR product for each sample was directly added to 1.5 µl of Cutsmart buffer (NEB), 0.2 µl of *Bsr*GI restriction enzyme (NEB), and 8.3 µl of nuclease-free H₂O. Samples were then incubated at 37 °C overnight, before alternate undigested and digested samples were loaded for gel electrophoresis.

To sequence *MSH1*, the region of interest was first amplified by PCR using primer set 2 (FP2: 5'TTGGACCCTAGCTTGAGGAA3', RP2: 5'ATCGAAGACCACCAAAAAGGA3') and Phusion high-fidelity DNA polymerase (NEB CAT#M0530S). PCR products were then purified using the QIAquick PCR Purification Kit (Qiagen) and sequenced from primer FP2 using an ABI 3730 capillary sequencer (Applied Biosystems).

Imaging and video analysis

Seedlings for imaging were sterilized, stratified, and grown on 50 µg ml⁻¹ kanamycin 1/2 MS plates as described above. After 4–5 d, seedlings were taken for imaging and, prior to mounting, stained with 10 µM propidium iodide (PI) solution for 3 min to capture the cell wall. Simple mounting of whole seedlings on microscope slides with coverslips was used (modified from Whelan and Murcha, 2015). In order to minimize the effects of hypoxia and physical stress on the seedling, imaging was undertaken in <10 min after the coverslip was added. For day/night experiments, care was taken to expose 'night' samples to as little light as possible during imaging sample preparation.

We used a Zeiss 710 laser scanning confocal microscope for imaging of seedlings. To characterize cells, we used an excitation wavelength of 543 nm, detection range 578–718 nm for both chlorophyll autofluorescence (peak emission 679.5 nm) and PI (peak emission 648 nm). For mitochondrial capture, we used an excitation wavelength of 488 nm, detection range 494–578 nm for GFP (peak emission 535.5 nm). Time-lapse images were taken, and all samples used in this study have the same time interval between frames, and the same length of capture, allowing for direct comparison.

For image analysis, single cells were cropped using the PI cell wall outline with Fiji (Image J 2.0.0). The universal length scale of 5 pixels µm⁻¹ was applied across all samples. To counter the occasional sample drift within time-lapse videos, drift correction was applied with default settings, using the cell outline via the PI channel as the stability landmark (Correct 3D drift, FIJI, ImageJ 2.1.0; Parslow *et al.*, 2014).

Following Chustecki *et al.* (2021), tracking of individual mitochondria was done using Trackmate (Tinevez *et al.*, 2017) in ImageJ 2.0.0. The LoG detector was used, with typical settings being 1 µm blob diameters (the typical size of a mitochondrion), although 0.8 µm was occasionally used for lower signal samples. The detection threshold was set between 1.5 and 8, and filters were applied on spots if necessary. The Simple LAP Tracker was run with a linking max distance of 4 µm (3 µm used for a few samples), gap-closing distance of 5 µm (4 µm used for a few samples), and gap-closing max frame gap of two frames. For each sample, the quality of overlaying detection for mitochondria was scrutinized, and occasional tracks were edited for precision.

Physical statistics

Speed (µm per frame) was computed as the distance moved per frame per trajectory. This value is averaged over all trajectories from the duration of the video. Inter-mitochondrial distance is the minimum Euclidean distance (µm) between every mitochondrion and its nearest physical neighbour in each frame. This value is averaged over all frames of the video. Co-localization time is the number of frames any two mitochondria have spent within a threshold distance (1.6 µm) of each other, averaged over all frames.

Mitochondrial morphology analysis was done with Fiji (Image J 2.0.0). Assessing mitochondrial size with fluorescence microscopy may be complicated by overexposure or other differences in signal intensity between samples. To introduce a technical control for exposure of GFP signal between the two genotypes, mtGFP samples were imaged at various gain values for the GFP channel. The images taken at exposures most comparable with the mtGFP-*msh1* images were then identified. This was achieved by comparing intensity distributions across mitochondrial regions and selecting the mtGFP set with the intensity distribution most comparable with mtGFP-*msh1*. In all cases, the mean intensity of mtGFP images selected in this way was within 5% of the mtGFP-*msh1* mean value. Area values (µm²) were then taken for mtGFP-*msh1* and selected mtGFP samples, by drawing selection regions around individual mitochondria that were not part of a cluster or directly adjacent to another individual.

Chloroplast co-localization analysis began with parallel tracking of the movement of mitochondria and chloroplasts over time in each

sample (Trackmate; [Tinevez et al., 2017](#)). Typical settings were the LoG detector using a blob diameter of 1–3 μm , with a detection threshold of 0.8–4, and filters applied on spots if necessary. Linking was done with the Simple LAP tracker with a linking distance of 3 μm or 4 μm , a gap closing distance of 3 μm or 4 μm , and a gap-closing max frame gap of two frames. Tracks were occasionally edited for precision before exporting.

We defined a statistic reporting the propensity of mitochondria to co-localize with chloroplasts beyond the co-localization that would be expected through a random arrangement of organelles. Co-localization ‘enrichment’ E is defined here as the ratio of mitochondrial density in chloroplast-adjacent regions to the density in non-adjacent regions, calculated per video frame as

$$E = (N_c/A_c) / [(N - N_c) / (A - A_c)]$$

Where N is the number of mitochondria in the current frame, A is the cell area estimate (μm^2), N_c is the number of mitochondria within distance d of the centre of the nearest chloroplast, where d is $2 \times 1.5 \mu\text{m}$ (twice the typical chloroplast radius). A_c is the estimate of available area of cell within distance d of the centre of a chloroplast (πd^2). E therefore reports the relative chloroplast-adjacent mitochondrial density with respect to chloroplast-distant density. Positional data were taken from mitochondrial and chloroplast trajectories as output from Trackmate.

Network statistics

Encounter networks are built from the close associations of mitochondria. A threshold distance of 1.6 μm was used to define a characteristic close association, being just over one mitochondrion’s length. Lower threshold distances can also be used, yielding fewer encounters, but similar connectivity trends ([Chustecki et al., 2021](#)). Networks build up as encounters (edges) between mitochondria (nodes) and are registered over time.

The mean degree is the number of immediate neighbours each node has, averaged over the number of nodes in the network. Network efficiency is the average, over all pairs of nodes, of the reciprocal shortest distance between each pair:

$$E(G) = \frac{1}{n(n-1)} \sum_{i \neq j \in G} \frac{1}{d(i,j)}$$

where G is the network of interest, n is the number of nodes in the network, and $d(i,j)$ is the distance (edge number) between node i and node j . The graph diameter is the length of the longest direct path across the network, a quantification of the number of edges connecting the two furthest nodes across a network. The mean graph betweenness centrality is the average number of shortest paths crossing each node in the network. The mean connected component number is the average number of disconnected subgraphs within the network.

Results

Construction, genotyping, and phenotyping of mtGFP-*msh1*

To allow the visualization of mitochondrial dynamics in the *msh1* mutant, we created mtGFP-*msh1*, combining the transgenic mtGFP line where GFP is localized to mitochondria [from an original line kindly provided by Professor David Logan ([Logan and Leaver, 2000](#))] with a mutant line where MSH1, an organelle genome maintenance factor, is perturbed

by a premature stop codon caused by an SNP ([Abdelnoor et al., 2003](#); see the Materials and methods for more details). We verified the crossed line using derived cleaved amplified polymorphic sequence (dCAPS) genotyping for the SNP and rosette phenotyping for characteristic variegation in the *msh1* line ([Supplementary Fig. S1](#)), where in contrast to both wild-type mtGFP and Col-0, mtGFP-*msh1* retained the expected variegated and low growth phenotype of the *msh1* mutant ([Supplementary Fig. 2A–C](#)). The candidate line at F₃ showed the presence of the SNP ([Supplementary Fig. S1A](#)), as well as resistance to kanamycin, demonstrating the presence of the mtGFP transgene ([Logan and Leaver, 2000](#)). Sequencing of the F₃ candidate line confirmed the presence of the SNP in the region encoding MSH1 ([Supplementary Fig. S3](#)). Sequencing of three F₄ candidate line offspring also showed the presence of the SNP, validating the genetic makeup of the mtGFP-*msh1* mutant.

msh1 alters physical dynamics of mitochondria

Following the creation of mtGFP-*msh1*, we used confocal microscopy to characterize mitochondrial dynamics in single hypocotyl cells of 4- to 5-day-old seedlings in this mutant, and compared these dynamics with those of the mtGFP transgenic line, representing wild-type mitochondrial motion. This imaging approach followed the protocol from [Chustecki et al. \(2021\)](#). Briefly, we recorded time-lapse videos of mitochondrial motion in single cells, and computationally identified trajectories of individual mitochondria using TrackMate ([Tinevez et al., 2017](#)). From these trajectories, we can analyse individual and collective behaviour of mitochondria, including speeds, co-localizations, and many more statistics ([Chustecki et al., 2021](#)). [Figure 1](#) illustrates the process of tracking fluorescent mitochondria over time, in representative mtGFP ([Fig. 1Ai](#)) and mtGFP-*msh1* ([Fig. 1Bi](#)) single cells. Generally and qualitatively, as with wild-type mtGFP mitochondrial motion, mtGFP-*msh1* mitochondria showed a mixture of diffusive and ballistic motion, with some organelles remaining static, and others moving swiftly across the cell. These organelles also co-localize with one another, and occasionally co-localize with chloroplasts ([Supplementary Video S1](#)).

We found that mitochondria in mtGFP-*msh1* on average were less evenly spread and were physically associated for longer times in hypocotyl cells ([Fig. 2](#)). Mean inter-mitochondrial distance, reporting the average distance (in microns) to the nearest physical neighbour in the cell, was lower in mtGFP-*msh1*, reflecting a less evenly spread population ([Fig. 2A](#)). The median speed of individual mitochondria in mtGFP-*msh1* was also lower, although differences between the lines did not cross a significance threshold when we used a conservative non-parametric test ([Fig. 2B](#)). Co-localization time, reporting the time over which two mitochondria are within a threshold of each other, was higher in mtGFP-*msh1* ([Fig. 2C](#)). Other physical and temporal aspects of mitochondrial

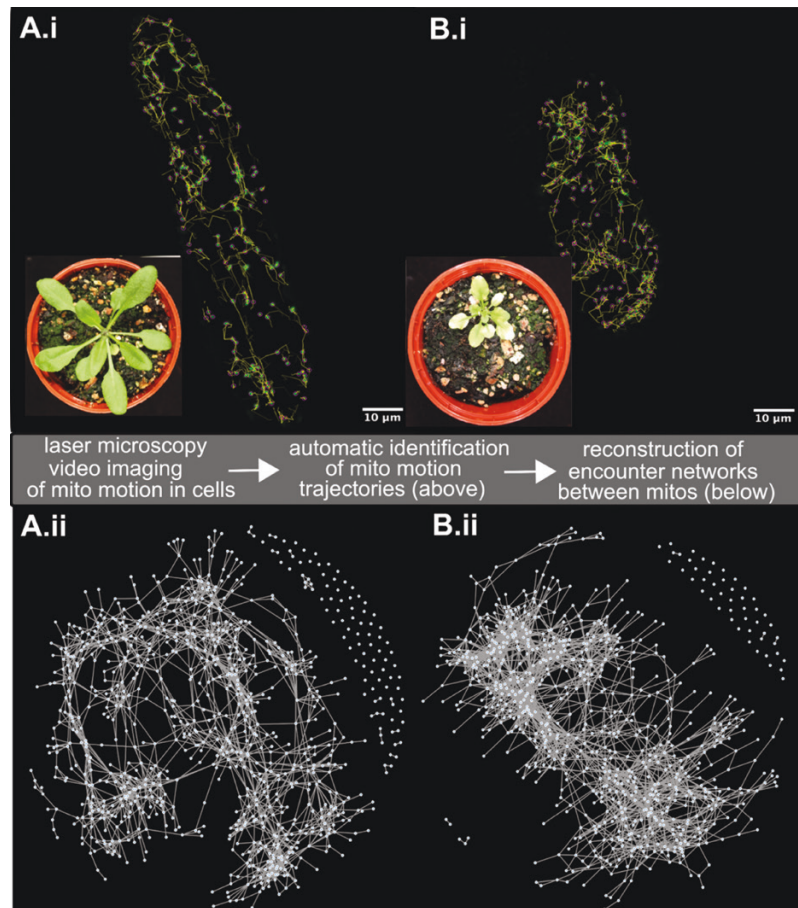


Fig. 1. Characterizing the ‘social networks’ of plant mitochondria in mtGFP (A) and mtGFP-*msh1* (B). Top panels (i) illustrate the tracking process of (green) fluorescent mitochondria in single hypocotyl cells from seedlings, using Trackmate (Tinevez *et al.*, 2017). Mitochondria are automatically identified (pink spots, diameter 1 μm), and computed tracks over time are shown [for clarity, only 10 local frames are shown (yellow)]. Insets show whole-plant phenotypes of the two lines later in development. Bottom panels (ii) show the networks of mitochondrial encounters corresponding to the single-cell dynamics (nodes are mitochondria, edges are encounters), built up over a time window of observation (here 233 s).

behaviour were not dramatically different in the *msh1* mutant. Cell sizes were similar across all lines (Supplementary Fig. S4), suggesting that these physical differences are intrinsic properties of the mitochondrial population and not a result of altered cellular morphology. Mitochondrial dynamics did not differ substantially when observed in night and day cycles either within or between either genotype (Supplementary Fig. S5A–G). We did observe a small change in individual mitochondrial area: *msh1* mitochondria were slightly smaller (Supplementary Fig. S5H, I). An increase in mitochondrial size in white (variegated) tissue in the *msh1* mutant has been previously observed (Xu *et al.*, 2011), reflecting a different direction of effect in tissue with a presumably different metabolic poise from the hypocotyl cells we consider. The propensity of mitochondria to co-localize with chloroplasts—measured as the relative density of mitochondria in chloroplast-adjacent to chloroplast-distant regions (see the Materials and methods)—did not significantly change between genotypes (Supplementary Fig. S5J). As always, absence of evidence for effects here cannot be interpreted as

evidence of absence of an effect, and these features may in fact differ between genotypes—but the scale of these differences was not large enough to be detectable here, suggesting that the collective physical dynamics we observe are the larger magnitude effect. The changes in collective behaviour that we do observe are thus compatible with our hypothesis that the cell sacrifices physical spacing (to favour organelle encounters allowing exchange of contents) in the *msh1* mutant.

Alterations in physical dynamics of msh1 affect social dynamics

To explore whether this change in spacing could indeed facilitate inter-mitochondrial connectivity, we next characterized the ‘encounter networks’ of mitochondria, defined as the set of co-localizations between pairs of mitochondria that occur within a given time frame (see the Materials and methods, Fig. 1Aii, Bii; Supplementary Fig. S6). Akin to social networks, describing social interactions between individuals in a population,

these encounter networks shape the potential for beneficial exchange of contents across the mitochondrial population (Chustecki *et al.*, 2021).

Salient features of these encounter networks for potential exchange of mitochondrial contents are the degree distribution (the number of different mitochondria each mitochondrion encounters), the diameter of the network (the length in edges of the longest direct route across the network), and the network efficiency. This final quantity is the average of the reciprocal lengths of the shortest paths between each pair of mitochondria in the network. If all pairs of mitochondria are connected by short paths (facilitating exchange through the

network), reciprocal lengths, and network efficiency, are high. If some pairs are connected only by long paths, or are disconnected, reciprocal lengths and efficiency are low and information exchange is more challenging.

We found that the encounter networks of mtGFP-*msh1* had a higher mean degree and higher efficiency than the mtGFP line (representative of wild-type mitochondrial networks) (Fig. 3A, B). Mitochondria in the *msh1* mutant are thus more directly connected through encounters, facilitating easier exchange of contents. Network diameter is also shorter across mtGFP-*msh1* networks, again suggesting increased organelle connectivity; but we note the significant difference

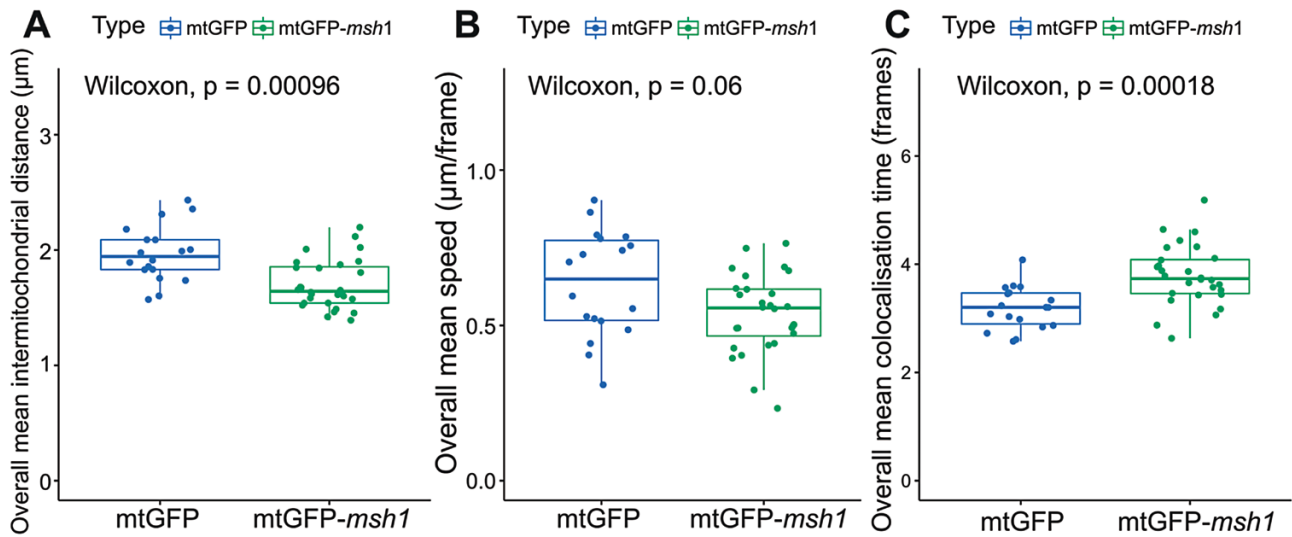


Fig. 2. Physical summary statistics differ between mtGFP and mtGFP-*msh1*. Each point represents a summary statistic for one cell (mtGFP $n=18$, mtGFP-*msh1* $n=28$). P -values represents outcome of the Wilcoxon rank sum test across both genotypes, without multiple hypothesis correction. Boxplots represent the median and 25th/75th percentile, with whiskers showing the smallest/largest value within $1.5\times$ the interquartile range. Each individual point gives the mean statistic across an entire video, corresponding to 233 s of video time.

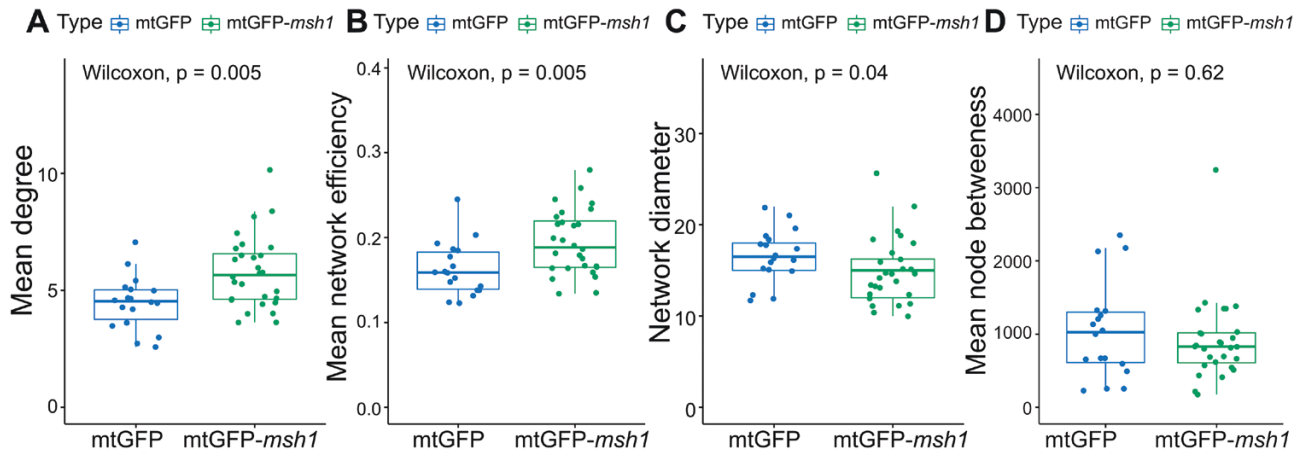


Fig. 3. Social summary statistics differ between mtGFP and mtGFP-*msh1*. Each point represents a summary statistic for one cell (mtGFP $n=18$, mtGFP-*msh1* $n=28$). P -values represents outcome of the Wilcoxon rank sum test across both genotypes, without multiple hypothesis correction. Boxplots represent the median and 25th/75th percentile, with whiskers showing the smallest/largest value within $1.5\times$ the interquartile range. Each individual point is from a network corresponding to an observed time window of 233 s.

was not retained after multiple hypothesis testing (Fig. 3C). The size of networks, quantified either by node or edge number, remained similar between mtGFP and mtGFP-*msh1* over time (Supplementary Fig. S7). There was no significant difference across values for betweenness centrality, an average of the number of shortest paths crossing each node in the network (Fig. 3D).

These network statistics are time dependent, because networks build up over time as more encounters between individuals occur. As seen in Supplementary Fig. S8, *msh1* differences in degree value remain across different observation time windows, with network efficiency differences significant at later frames (Fig. 3A, B; Supplementary Fig. S8A, B), when networks have built up with more encounters. Network diameter relationships across the lines do not substantially change over time, but betweenness centrality is significantly different for early comparisons between lines, although not at later frames (Fig. 3C, D; Supplementary Fig. S8C, D). This could be a consequence of the topology of smaller networks, before so many encounters and connections between smaller cliques of mitochondria are formed.

Taken together with the physical results, these observations support our hypothesis that the genetic challenge provided by the *msh1* mutation can invoke a compensatory shift in mitochondrial dynamics, sacrificing physical spacing to facilitate more organelle encounters, which may in turn support more efficient exchange of contents.

The collective dynamic response to msh1 resembles the response to friendly

We next asked whether the altered mitochondrial behaviour in the face of the *msh1* perturbation shared similarities with altered behaviour under a physical perturbation to mitochondrial dynamics. To this end, we characterized an mtGFP-*friendly* mutant within which the fusion of these organelles is perturbed (El Zawily *et al.*, 2014), increasing the association time between individuals, and posing a transient challenge to the social connectivity and physical spread trade-off as shown in Chustecki *et al.* (2021). Recent work has illuminated the co-localization of FRIENDLY to depolarized mitochondria as an essential part of the mitophagy pathway (Ma *et al.*, 2021); its perturbation results in reduced mitochondrial fusion, increased mitochondrial clustering, and a wide range of metabolic issues (El Zawily *et al.*, 2014; Ma *et al.*, 2021). This mutant has a pronounced growth phenotype, though more limited than *msh1* (Supplementary Fig. S2D).

To explore the relationship between changes in mitochondrial behaviour due to physical and genetic challenges, we compared mitochondrial behaviour in mtGFP, mtGFP-*msh1*, and mtGFP-*friendly*. Strikingly, the physical and social statistics observed in mtGFP-*msh1* and mtGFP-*friendly* lines are remarkably similar, with no statistically detectable differences

between these genotypes. Of course, an absence of statistical significance does not imply the absence of an effect, but the observed magnitudes of the statistics and our moderate sample sizes ($n=28$ for mtGFP-*msh1*, $n=19$ for mtGFP-*friendly*) suggest that the behaviours are indeed rather similar (Fig. 4). There was a slightly lower inter-mitochondrial distance alongside an increased degree and network efficiency within mtGFP-*msh1*—suggesting a marginally more pronounced shift towards connectivity—although these observations did not meet a statistical significance threshold for a non-parametric comparison (Fig. 4A, D, E). Both mutant genotypes show a significantly decreased inter-mitochondrial distance, and increased co-localization time and degree, when compared with wild-type mtGFP (Fig. 4A, C, D).

Previous work (Chustecki *et al.*, 2021) found that the difference between mtGFP-*friendly* and wild-type behaviour diminished over time: initially rather cliquey, the *friendly* networks became more globally connected over time as itinerant mitochondria formed social bridges between cliques. Our statistical analysis here supports this picture for mean degree in both *friendly* and *msh1* (Fig. 4D; Supplementary Fig. S8A) while revealing a more nuanced picture for other network statistics. In particular, network efficiency differences between the mutants and wild type do not diminish over time to the same extent (Fig. 4E; Supplementary Fig. S8B), suggesting that the global changes in collective behaviour are maintained robustly over time despite similarities in local behaviour. Overall, both the magnitudes and time behaviour of collective dynamic changes were quantitatively similar in *friendly* and *msh1*, supporting the comparable influences of the two perturbations.

Discussion

Mitochondria across eukaryotes are strikingly dynamic. In some cases, including the delivery of ATP to synapses in neurons (Hollenbeck and Saxton, 2005; Mironov, 2007; MacAskill *et al.*, 2010) and of fit mitochondria to growing buds in yeast (Fehrenbacher *et al.*, 2004; Pernice *et al.*, 2018), the reasons for this motion are largely explained. In many other cases, the advantages and disadvantages of the rich dynamics of mitochondria remain unclear. Here we have demonstrated that a perturbation to nuclear-encoded machinery responsible for mtDNA maintenance influences the collective physical dynamics of plant mitochondria in such a way as to trade reduced spacing for increased connectivity. In turn, we suggest that this increased capacity for interaction may support more mtDNA sharing and complementation in the face of compromised mtDNA (Fig. 5), as well as increased potential exchange of other chemicals. Strikingly, this response of collective dynamics to a genetic challenge resembles that to a physical challenge (induced by the *friendly* mutation), underlining the link between genetic and physical dynamics of mitochondrial populations.

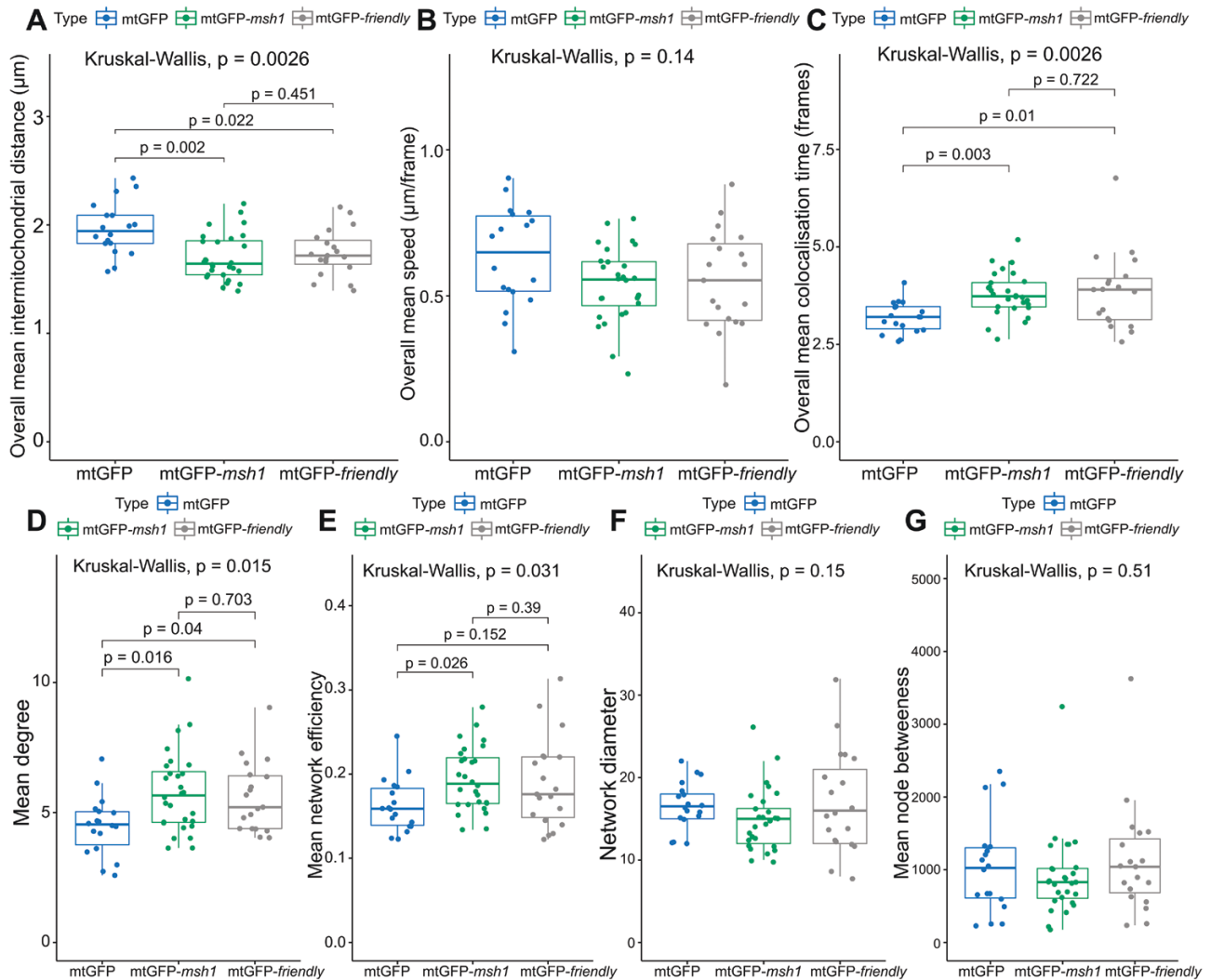


Fig. 4. Physical and social summary statistics compared across mtGFP, mtGFP-*msh1*, and *friendly*. Each point represents a summary statistic for one cell (mtGFP $n=18$, mtGFP-*msh1* $n=28$, *friendly* $n=19$). P -values represent Kruskal–Wallis test outcomes across all three genotypes, and pairwise P -values are false discovery rate-adjusted outcomes of a post-hoc Dunn test, without multiple hypothesis correction across statistics. Boxplots represent the median and 25th/75th percentile, with whiskers showing the smallest/largest value within $1.5\times$ the interquartile range. Each physical datapoint (A–C) is a mean across a 233 s time window, and each social datapoint (D–G) is from a network corresponding to a time window of 233 s.

msh1 mutants demonstrate an increase in single nucleotide variants and insertion–deletion mutations (Wu *et al.*, 2020), as the protein forms part of the mtDNA damage repair machinery (Davila *et al.*, 2011; Christensen, 2014; Gualberto *et al.*, 2014; Wu *et al.*, 2020). In other plants, although not in *Arabidopsis*, substoichiometric shifting due to MSH1 disruption also leads to cytoplasmic male sterility (Arrieta-Montiel *et al.*, 2001; Sandhu *et al.*, 2007; Xu *et al.*, 2011; Viridi *et al.*, 2016)—a substantial biological challenge (although one of value in crop breeding). The increased connectivity we observe across the chondriome could provide individual mitochondria with a chance to access undamaged mtDNA, or extra copies of gene sequences to use as guide strands during double-strand break repair. One potentially quite general principle is that the physical dynamics of organelles exert control on the genetic

dynamics of organellar DNA, and the cell can thus address genetic priorities by controlling physical behaviour (Johnston, 2019). However, other effects of the *msh1* mutation may also play roles in shaping the collective dynamic response, including metabolic influence from mitochondrial and chloroplast dysfunction, transgenerational subtleties of mtDNA mutations and nuclear DNA methylation, and consequent or independent influences on the internal structure of the cell. Further work characterizing mitochondrial collective dynamics in lines controlling for these influences will help provide further support for the physical–genetic feedback hypothesis.

Other examples exist of where plant mitochondrial dynamics may influence mtDNA genetic structure. In the SAM, a cage-like mitochondrial network has been observed to form (Seguí-Simarro and Staehelin, 2009), in contrast to the largely

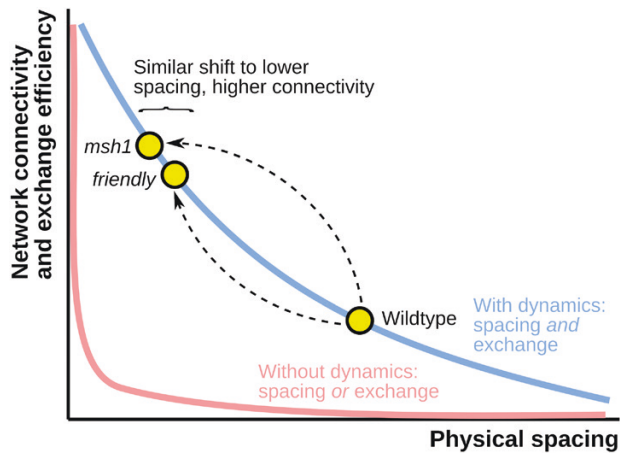


Fig. 5. Different resolutions to the social/spacing trade-off. There exists a trade-off (coloured curves) between physical spacing of mitochondria (horizontal axis) and the connectivity of the chondriome (vertical axis). Without mitochondrial dynamics, static organelles are either co-localized or spaced, with little capacity to support both behaviours together (pink). Mitochondrial dynamics provides a resolution: as organelles move, they can transiently co-localize while usually remaining spaced (blue), allowing some capacity for both behaviours. Wild-type Arabidopsis adopts a particular balance between spacing and encounters. This balance is shifted in the *msh1* mutant, where mitochondria sacrifice spacing and increase inter-mitochondrial encounters. This increased ‘social’ connectivity may support fusion, exchange, and complementation of damaged mtDNA. *friendly* mutants reflect a similar shift in balance, caused by a physical perturbation.

individual mitochondria observed in other tissues. This network structure allows mtDNA mixing and facilitates recombination (Edwards *et al.*, 2021; Rose, 2021). In conjunction with this physical change, relative expression of MSH1 is particularly high in the SAM, which may both assist with maintenance and support germline mtDNA segregation through gene conversion as an evolutionary priority (Schmid *et al.*, 2005; Edwards *et al.*, 2021; Broz *et al.*, 2022).

Other tissues where mitochondrial dynamics have been characterized include leaves (where the tight packing of chloroplasts means that mitochondria are extremely constrained), cotyledon [where mitochondrial collective dynamics resemble those observed in hypocotyl (Arimura *et al.*, 2004; Chustecki *et al.*, 2021)], and root epidermis [where some cells appear to have relatively stationary mitochondrial populations, and others have collective dynamics that again resemble those in hypocotyl (Logan and Leaver, 2000; Zheng *et al.*, 2009)—including in response to the *friendly* mutant (El Zawily *et al.*, 2014)]. Speculatively, this suggests a picture where collective dynamics (under the constraints of cell structure) can contribute to mtDNA maintenance in similar ways in somatic tissues, while the above-ground germline reflects the completely connected extreme on the spectrum of connectivity and spacing (Fig. 5) due to the increased need for faithful mtDNA inheritance between generations (Logan, 2006b; Seguí-Simarro and Staehelin, 2009; Wolożyszynska, 2010; Johnston, 2019; Edwards *et al.*, 2021).

The link between the physical behaviour of mitochondria and the genetic behaviour of mtDNA is still being elucidated (Aryaman *et al.*, 2019; Johnston, 2019; Edwards *et al.*, 2021). The production, degradation, fission, fusion, partitioning, motion, and arrangement of mitochondria in the cell all influence the genetic structure of the mtDNA population. Mitochondria are increasingly being recognized as ‘social’ organelles, with their interactions playing important functional roles beyond what a collection of independent individuals could achieve (Picard and Sandi, 2021). In plants, a picture of collective behaviour emerging from a population of individuals is particularly pertinent, as mitochondria physically retain individual identities to a much greater extent than in other kingdoms where fused networks are common. The sharing of contents between mitochondria, and consequent control of contents throughout the population, is an example of such emergent behaviour that could not be achieved by independent organelles. Our results here demonstrate that the collective dynamics of mitochondria may respond to genetic challenges as well as physical challenges, suggesting that control of these dynamics may provide the cell with a way of exploiting the physical–genetic link in the face of genetic perturbation. Plant cells, with largely individual mitochondria readily visualized in a quasi-2D cytosolic domain, are an excellent model system for further exploring this link, and we believe that the encounter networks we characterize here will find further use in investigating the vital emergent collective dynamics of the chondriome.

Supplementary data

The following supplementary data are available at [JXB online](#).

Fig. S1. Genotyping for F₃ *msh1* homozygosity leads to consistently variegated F₄ progeny.

Fig. S2. Plant phenotypes reveal developmental differences across genotypes.

Fig. S3. Single nucleotide polymorphism in MSH1 retained in the F₃ generation of the mtGFP-*msh1* cross.

Fig. S4. No evidence found for a difference between median cell area across genotypes.

Fig. S5. Limited *msh1* influence on other temporal or spatial aspects of mitochondrial behaviour.

Fig. S6. Sample encounter networks for mtGFP and mtGFP-*msh1*.

Fig. S7. Node number and edge number of encounter networks did not vary greatly between lines for mtGFP, mtGFP-*msh1*, and mtGFP-*friendly*.

Fig. S8. Social summary statistics provide evidence of differences between mtGFP, mtGFP-*msh1*, and *friendly*, at three earlier times.

Video S1. Example mitochondrial dynamics in *msh1* hypocotyl.

Acknowledgements

We gratefully acknowledge the Imaging Suite (BALM) at the University of Birmingham for support of imaging experiments, and thank Alessandro di Maio and Professor Markus Schwarzländer for advice with design and analysis of imaging experiments. We are very grateful to Professor David Logan for mtGFP seeds. Thanks to Miguel Pachón Peñalba and Alice Darbyshire for molecular biology experimental advice and help in primer design. We gratefully acknowledge the services of Genomics at Birmingham for sequencing experiments.

Author contributions

IGJ: conceptualization and supervision of theoretical work; JMC: creating plant lines, performing microscopy, and statistical analysis; JMC and RDE: performing sequencing and validation; IGJ and DJG: supervision of laboratory work; IGJ and JMC: writing—draft. All authors edited the manuscript.

Conflict of interest

The authors declare that no competing interests exist.

Funding

JMC is supported by the BBSRC and University of Birmingham via the MIBTP doctoral training scheme (grant no. BB/M01116X/1). This project has received funding from the European Research Council (ERC) under the European Union's Horizon 2020 research and innovation programme [grant agreement nos 805046 (EvoConBio) to IGJ and 715441 (GasPlaNt) to DJG, and supporting RDE].

Data availability

All data and analysis codes are available from Github at <https://github.com/StochasticBiology/plant-mito-dynamics>

References

- Abdelnoor RV, Christensen AC, Mohammed S, Munoz-Castillo B, Moriyama H, Mackenzie SA. 2006. Mitochondrial genome dynamics in plants and animals: convergent gene fusions of a MutS homologue. *Journal of Molecular Evolution* **63**, 165–173. doi: [10.1007/s00239-005-0226-9](https://doi.org/10.1007/s00239-005-0226-9).
- Abdelnoor RV, Yule R, Elo A, Christensen AC, Meyer-Gauen G, Mackenzie SA. 2003. Substoichiometric shifting in the plant mitochondrial genome is influenced by a gene homologous to MutS. *Proceedings of the National Academy of Sciences, USA* **100**, 5968–5973. doi: [10.1073/pnas.1037651100](https://doi.org/10.1073/pnas.1037651100).
- Agrawal A, Pekkurnaz G, Koslover EF. 2018. Spatial control of neuronal metabolism through glucose-mediated mitochondrial transport regulation. *eLife* **7**, e40986. doi: [10.7554/eLife.40986](https://doi.org/10.7554/eLife.40986).
- Arimura S-i, Yamamoto J, Aida GP, Nakazono M, Tsutsumi N. 2004. Frequent fusion and fission of plant mitochondria with unequal nucleoid distribution. *Proceedings of the National Academy of Sciences, USA* **101**, 7805–7808. doi: [10.1073/pnas.0401077101](https://doi.org/10.1073/pnas.0401077101).
- Arrieta-Montiel M, Lyznik A, Woloszynska M, Janska H, Töhme J, Mackenzie S. 2001. Tracing evolutionary and developmental implications of mitochondrial stoichiometric shifting in the common bean. *Genetics* **158**, 851–864. doi: [10.1093/genetics/158.2.851](https://doi.org/10.1093/genetics/158.2.851).
- Arrieta-Montiel MP, Shedje V, Davila J, Christensen AC, Mackenzie SA. 2009. Diversity of the Arabidopsis mitochondrial genome occurs via nuclear-controlled recombination activity. *Genetics* **183**, 1261–1268. doi: [10.1534/genetics.109.108514](https://doi.org/10.1534/genetics.109.108514).
- Aryaman J, Bowles C, Jones NS, Johnston IG. 2019. Mitochondrial network state scales mtDNA genetic dynamics. *Genetics* **212**, 1429–1443. doi: [10.1534/genetics.119.302423](https://doi.org/10.1534/genetics.119.302423).
- Barton KA, Wozny MR, Mathur N, Jaipargas E-A, Mathur J. 2018. Chloroplast behaviour and interactions with other organelles in *Arabidopsis thaliana* pavement cells. *Journal of Cell Science* **131**, jcs202275. doi: [10.1242/jcs.202275](https://doi.org/10.1242/jcs.202275).
- Bauwe H, Hagemann M, Fernie AR. 2010. Photorespiration: players, partners and origin. *Trends in Plant Science* **15**, 330–336. doi: [10.1016/j.tplants.2010.03.006](https://doi.org/10.1016/j.tplants.2010.03.006).
- Bellaoui M, Martin-Canadell A, Pelletier G, Budar F. 1998. Low-copy-number molecules are produced by recombination, actively maintained and can be amplified in the mitochondrial genome of Brassicaceae: relationship to reversion of the male sterile phenotype in some cybrids. *Molecular & General Genetics* **257**, 177–185. doi: [10.1007/S004380050637](https://doi.org/10.1007/S004380050637).
- Belliard G, Vedel F, Pelletier G. 1979. Mitochondrial recombination in cytoplasmic hybrids of *Nicotiana tabacum* by protoplast fusion. *Nature* **281**, 401–403. doi: [10.1038/281401a0](https://doi.org/10.1038/281401a0).
- Browse J, McConn M, James D, Miquel M. 1993. Mutants of Arabidopsis deficient in the synthesis of α -linolenate. *Journal of Biological Chemistry* **268**, 16345–16351. doi: [10.1016/s0021-9258\(19\)85427-3](https://doi.org/10.1016/s0021-9258(19)85427-3).
- Broz AK, Keene A, Gyorfy MF, Hodous M, Johnston IG, Sloan DB. 2022. Sorting mitochondrial and plastid heteroplasmy in Arabidopsis is extremely rapid and depends on MSH1 activity. *Proc Natl Acad Sci USA* **119**, e2206973119. doi: [10.1073/pnas.2206973119](https://doi.org/10.1073/pnas.2206973119).
- Chen H, Chan DC. 2006. Critical dependence of neurons on mitochondrial dynamics. *Current Opinion in Cell Biology* **18**, 453–459. doi: [10.1016/j.ceb.2006.06.004](https://doi.org/10.1016/j.ceb.2006.06.004).
- Christensen AC. 2014. Genes and junk in plant mitochondria—repair mechanisms and selection. *Genome Biology and Evolution* **6**, 1448–1453. doi: [10.1093/gbe/evu115](https://doi.org/10.1093/gbe/evu115).
- Chustecki JM, Gibbs DJ, Bassel GW, Johnston IG. 2021. Network analysis of Arabidopsis mitochondrial dynamics reveals a resolved tradeoff between physical distribution and social connectivity. *Cell Systems* **12**, 419–431. doi: [10.1016/j.cels.2021.04.006](https://doi.org/10.1016/j.cels.2021.04.006).
- Davila JI, Arrieta-Montiel MP, Wamboldt Y, Cao J, Hagemann J, Shedje V, Xu YZ, Weigel D, Mackenzie SA. 2011. Double-strand break repair processes drive evolution of the mitochondrial genome in Arabidopsis. *BMC Biology* **9**, 1–14. doi: [10.1186/1741-7007-9-64](https://doi.org/10.1186/1741-7007-9-64).
- Edwards DM, Røyrvik EC, Chustecki JM, Giannakis K, Glastad RC, Radzvilavicius AL, Johnston IG. 2021. Avoiding organelle mutational meltdown across eukaryotes with or without a germline bottleneck. *PLoS Biology* **19**, e3001153. doi: [10.1371/journal.pbio.3001153](https://doi.org/10.1371/journal.pbio.3001153).
- El Zawily AM, Schwarzländer M, Finkemeier I, et al. 2014. FRIENDLY regulates mitochondrial distribution, fusion, and quality control in Arabidopsis. *Plant Physiology* **166**, 808–828. doi: [10.1104/pp.114.243824](https://doi.org/10.1104/pp.114.243824).
- Fehrenbacher KL, Yang HC, Gay AC, Huckaba TM, Pon LA. 2004. Live cell imaging of mitochondrial movement along actin cables in budding yeast. *Current Biology* **14**, 1996–2004. doi: [10.1016/J.CUB.2004.11.004](https://doi.org/10.1016/J.CUB.2004.11.004).
- Figge MT, Reichert AS, Meyer-Hermann M, Osiewicz HD. 2012. Deceleration of fusion-fission cycles improves mitochondrial quality control during aging. *PLoS Computational Biology* **8**, 1002576. doi: [10.1371/journal.pcbi.1002576](https://doi.org/10.1371/journal.pcbi.1002576).
- Fukui K, Harada A, Wakamatsu T, Minobe A, Ohshita K, Ashiuchi M, Yano T. 2018. The GIY–YIG endonuclease domain of Arabidopsis MutS homolog 1 specifically binds to branched DNA structures. *FEBS Letters* **592**, 4066–4077. doi: [10.1002/1873-3468.13279](https://doi.org/10.1002/1873-3468.13279).

- Gualberto JM, Mileshina D, Wallet C, Niazi AK, Weber-Lotfi F, Dietrich A.** 2014. The plant mitochondrial genome: dynamics and maintenance. *Biochimie* **100**, 107–120. doi: [10.1016/j.biochi.2013.09.016](https://doi.org/10.1016/j.biochi.2013.09.016).
- Gualberto JM, Newton KJ.** 2017. Plant mitochondrial genomes: dynamics and mechanisms of mutation. *Annual Review of Plant Biology* **68**, 225–252. doi: [10.1146/annurev-arplant-043015-112232](https://doi.org/10.1146/annurev-arplant-043015-112232).
- Hollenbeck PJ, Saxton WM.** 2005. The axonal transport of mitochondria. *Journal of Cell Science* **118**, 5411–5419. doi: [10.1242/JCS.02745](https://doi.org/10.1242/JCS.02745).
- Ichas F, Jouaville LS, Mazat JP.** 1997. Mitochondria are excitable organelles capable of generating and conveying electrical and calcium signals. *Cell* **89**, 1145–1153. doi: [10.1016/S0092-8674\(00\)80301-3](https://doi.org/10.1016/S0092-8674(00)80301-3).
- Islam MS, Niwa Y, Takagi S.** 2009. Light-dependent intracellular positioning of mitochondria in *Arabidopsis thaliana* mesophyll cells. *Plant & Cell Physiology* **50**, 1032–1040. doi: [10.1093/pcp/pcp054](https://doi.org/10.1093/pcp/pcp054).
- Islam MS, Van Nguyen T, Sakamoto W, Takagi S.** 2020. Phototropin- and photosynthesis-dependent mitochondrial positioning in *Arabidopsis thaliana* mesophyll cells. *Journal of Integrative Plant Biology* **62**, 1352–1371. doi: [10.1111/jipb.12910](https://doi.org/10.1111/jipb.12910).
- Jaipargas E-A, Barton KA, Mathur N, Mathur J.** 2015. Mitochondrial pleomorphy in plant cells is driven by contiguous ER dynamics. *Frontiers in Plant Science* **6**, 783. doi: [10.3389/fpls.2015.00783](https://doi.org/10.3389/fpls.2015.00783).
- Johnston IG.** 2019. Tension and resolution: dynamic, evolving populations of organelle genomes within plant cells. *Molecular Plant* **12**, 764–783. doi: [10.1016/j.molp.2018.11.002](https://doi.org/10.1016/j.molp.2018.11.002).
- Jones DP.** 1986. Intracellular diffusion gradients of O₂ and ATP. *American Journal of Physiology* **250**, C663–C675. doi: [10.1152/AJPCELL.1986.250.5.C663](https://doi.org/10.1152/AJPCELL.1986.250.5.C663).
- Karbowski M, Youle RJ.** 2003. Dynamics of mitochondrial morphology in healthy cells and during apoptosis. *Cell Death and Differentiation* **10**, 870–880. doi: [10.1038/sj.cdd.4401260](https://doi.org/10.1038/sj.cdd.4401260).
- Klepikova A, Kasianov A, Gerasimov E, Logacheva M, Penin A.** 2016. A high resolution map of the *Arabidopsis thaliana* developmental transcriptome based on RNA-seq profiling. *The Plant Journal* **88**, 1058–1070. doi: [10.1111/TPJ.13312](https://doi.org/10.1111/TPJ.13312).
- Kozik A, Rowan BA, Lavelle D, Berke L, Schranz ME, Michelmore RW, Christensen AC.** 2019. The alternative reality of plant mitochondrial DNA: one ring does not rule them all. *PLoS Genetics* **15**, e1008373. doi: [10.1371/journal.pgen.1008373](https://doi.org/10.1371/journal.pgen.1008373).
- Krupinska K, Blanco NE, Oetke S, Zottini M.** 2020. Genome communication in plants mediated by organelle–nucleus-located proteins. *Philosophical Transactions of the Royal Society B: Biological Sciences* **375**, 20190397. doi: [10.1098/rstb.2019.0397](https://doi.org/10.1098/rstb.2019.0397).
- Liesa M, Shirihai OS.** 2013. Mitochondrial dynamics in the regulation of nutrient utilization and energy expenditure. *Cell Metabolism* **17**, 491–506. doi: [10.1016/j.cmet.2013.03.002](https://doi.org/10.1016/j.cmet.2013.03.002).
- Liu X, Weaver D, Shirihai O, Hajnóczky G.** 2009. Mitochondrial ‘kiss-and-run’: interplay between mitochondrial motility and fusion–fission dynamics. *The EMBO Journal* **28**, 3074–3089. doi: [10.1038/emboj.2009.255](https://doi.org/10.1038/emboj.2009.255).
- Logan DC.** 2006a. Plant mitochondrial dynamics. *Biochimica et Biophysica Acta* **1763**, 430–441. doi: [10.1016/j.bbamcr.2006.01.003](https://doi.org/10.1016/j.bbamcr.2006.01.003).
- Logan DC.** 2006b. The mitochondrial compartment. *Journal of Experimental Botany* **57**, 1225–1243. doi: [10.1093/jxb/erj151](https://doi.org/10.1093/jxb/erj151).
- Logan DC.** 2010. The dynamic plant chondriome. *Seminars in Cell and Developmental Biology* **21**, 550–557. doi: [10.1016/j.semcdb.2009.12.010](https://doi.org/10.1016/j.semcdb.2009.12.010).
- Logan DC, Leaver CJ.** 2000. Mitochondria-targeted GFP highlights the heterogeneity of mitochondrial shape, size and movement within living plant cells. *Journal of Experimental Botany* **51**, 865–871. doi: [10.1093/jxb/51.346.865](https://doi.org/10.1093/jxb/51.346.865).
- Lonsdale DM, Brears T, Hodge TP, Melville SE, Rottmann WH.** 1988. The plant mitochondrial genome: homologous recombination as a mechanism for generating heterogeneity. *Philosophical Transactions of the Royal Society B: Biological Sciences* **319**, 149–163. doi: [10.1098/rstb.1988.0039](https://doi.org/10.1098/rstb.1988.0039).
- Ma J, Liang Z, Zhao J, et al.** 2021. Friendly mediates membrane depolarization-induced mitophagy in *Arabidopsis*. *Current Biology* **31**, 1931–1944. doi: [10.1016/j.cub.2021.02.034](https://doi.org/10.1016/j.cub.2021.02.034).
- MacAskill AF, Atkin TA, Kittler JT.** 2010. Mitochondrial trafficking and the provision of energy and calcium buffering at excitatory synapses. *European Journal of Neuroscience* **32**, 231–240. doi: [10.1111/J.1460-9568.2010.07345.X](https://doi.org/10.1111/J.1460-9568.2010.07345.X).
- Martínez-Zapater JM, Gil P, Capel J, Somerville CR.** 1992. Mutations at the *Arabidopsis* CHM locus promote rearrangements of the mitochondrial genome. *The Plant Cell* **4**, 889–899. doi: [10.1105/tpc.4.8.889](https://doi.org/10.1105/tpc.4.8.889).
- Mironov SL.** 2007. ADP regulates movements of mitochondria in neurons. *Biophysical Journal* **92**, 2944–2952. doi: [10.1529/BIOPHYSJ.106.092981](https://doi.org/10.1529/BIOPHYSJ.106.092981).
- Nakabayashi K, Okamoto M, Koshiba T, Kamiya Y, Nambara E.** 2005. Genome-wide profiling of stored mRNA in *Arabidopsis thaliana* seed germination: epigenetic and genetic regulation of transcription in seed. *The Plant Journal* **41**, 697–709. doi: [10.1111/J.1365-313X.2005.02337.X](https://doi.org/10.1111/J.1365-313X.2005.02337.X).
- Neff MM, Neff JD, Chory J, Pepper AE.** 1998. dCAPS, a simple technique for the genetic analysis of single nucleotide polymorphisms: experimental applications in *Arabidopsis thaliana* genetics. *The Plant Journal* **14**, 387–392. doi: [10.1046/j.1365-313X.1998.00124.x](https://doi.org/10.1046/j.1365-313X.1998.00124.x).
- Parslow A, Cardona A, Bryson-Richardson RJ.** 2014. Sample drift correction following 4D confocal time-lapse imaging. *Journal of Visualized Experiments* **86**, 51086. doi: [10.3791/51086](https://doi.org/10.3791/51086).
- Pernice WM, Swayne TC, Boldogh IR, Pon LA.** 2018. Mitochondrial tethers and their impact on lifespan in budding yeast. *Frontiers in Cell and Developmental Biology* **5**, 120. doi: [10.3389/fcell.2017.00120](https://doi.org/10.3389/fcell.2017.00120).
- Picard M, McManus MJ, Csordás G, Várnai P, Dorn GW, Williams D, Hajnóczky G, Wallace DC.** 2015. Trans-mitochondrial coordination of cristae at regulated membrane junctions. *Nature Communications* **6**, 6259. doi: [10.1038/ncomms7259](https://doi.org/10.1038/ncomms7259).
- Picard M, Sandi C.** 2021. The social nature of mitochondria: implications for human health. *Neuroscience and Biobehavioral Reviews* **120**, 595–610. doi: [10.1016/j.neubiorev.2020.04.017](https://doi.org/10.1016/j.neubiorev.2020.04.017).
- Preuten T, Cincu E, Fuchs J, Zoschke R, Liere K, Börner T.** 2010. Fewer genes than organelles: extremely low and variable gene copy numbers in mitochondria of somatic plant cells. *The Plant Journal* **64**, 948–959. doi: [10.1111/j.1365-313X.2010.04389.x](https://doi.org/10.1111/j.1365-313X.2010.04389.x).
- Rédei GP.** 1973. Extra-chromosomal mutability determined by a nuclear gene locus in *Arabidopsis*. *Mutation Research* **18**, 149–162. doi: [10.1016/0027-5107\(73\)90031-6](https://doi.org/10.1016/0027-5107(73)90031-6).
- Rose RJ.** 2021. Contribution of massive mitochondrial fusion and subsequent fission in the plant life cycle to the integrity of the mitochondrion and its genome. *International Journal of Molecular Sciences* **22**, 5429. doi: [10.3390/ijms22115429](https://doi.org/10.3390/ijms22115429).
- Sage RF, Sage TL, Kocacinar F.** 2012. Photorespiration and the evolution of C₄ photosynthesis. *Annual Review of Plant Biology* **63**, 19–47. doi: [10.1146/annurev-arplant-042811-105511](https://doi.org/10.1146/annurev-arplant-042811-105511).
- Sakamoto W, Arrieta-Montiel M, Christensen AC, Mackenzie SA.** 1996. Altered mitochondrial gene expression in a maternal distorted leaf mutant of *Arabidopsis* induced by chloroplast mutator. *The Plant Cell* **8**, 1377–1390. doi: [10.1105/tpc.8.8.1377](https://doi.org/10.1105/tpc.8.8.1377).
- Sandhu APS, Abdelnoor RV, Mackenzie SA.** 2007. Transgenic induction of mitochondrial rearrangements for cytoplasmic male sterility in crop plants. *Proceedings of the National Academy of Sciences, USA* **104**, 1766–1770. doi: [10.1073/pnas.0609344104](https://doi.org/10.1073/pnas.0609344104).
- Santo-Domingo J, Giacomello M, Poburko D, Scorrano L, Demarex N.** 2013. OPA1 promotes pH flashes that spread between contiguous mitochondria without matrix protein exchange. *The EMBO Journal* **32**, 1927–1940. doi: [10.1038/emboj.2013.124](https://doi.org/10.1038/emboj.2013.124).
- Schmid M, Davison T, Henz S, Pape U, Demar M, Vingron M, Schölkopf B, Weigel D, Lohmann J.** 2005. A gene expression map of *Arabidopsis thaliana* development. *Nature Genetics* **37**, 501–506. doi: [10.1038/NG1543](https://doi.org/10.1038/NG1543).
- Schuler MH, Lewandowska A, Di Caprio G, Skillern W, Upadhyayula S, Kirchhausen T, Shaw JM, Cunniff B.** 2017. Miro1-mediated mitochondrial positioning shapes intracellular energy gradients required for cell migration. *Molecular Biology of the Cell* **28**, 2159–2169. doi: [10.1091/mbc.E16-10-0741](https://doi.org/10.1091/mbc.E16-10-0741).

- Seguí-Simarro JM, Staehelin LA.** 2009. Mitochondrial reticulation in shoot apical meristem cells of Arabidopsis provides a mechanism for homogenization of mtDNA prior to gamete formation. *Plant Signaling & Behavior* **4**, 168–171. doi: [10.4161/psb.4.3.7755](https://doi.org/10.4161/psb.4.3.7755).
- Shai N, Schuldiner M, Zalckvar E.** 2016. No peroxisome is an island—peroxisome contact sites. *Biochimica et Biophysica Acta* **1863**, 1061–1069. doi: [10.1016/j.bbamcr.2015.09.016](https://doi.org/10.1016/j.bbamcr.2015.09.016).
- Shao MR, Kumar Kenchanmane Raju S, Laurie JD, Sanchez R, Mackenzie SA.** 2017. Stress-responsive pathways and small RNA changes distinguish variable developmental phenotypes caused by MSH1 loss. *BMC Plant Biology* **17**, 47. doi: [10.1186/s12870-017-0996-4](https://doi.org/10.1186/s12870-017-0996-4).
- Sheahan MB, McCurdy DW, Rose RJ.** 2005. Mitochondria as a connected population: ensuring continuity of the mitochondrial genome during plant cell dedifferentiation through massive mitochondrial fusion. *The Plant Journal* **44**, 744–755. doi: [10.1111/j.1365-313X.2005.02561.x](https://doi.org/10.1111/j.1365-313X.2005.02561.x).
- Shedge V, Arrieta-Montiel M, Christensen AC, Mackenzie SA.** 2007. Plant mitochondrial recombination surveillance requires unusual RecA and MutS homologs. *The Plant Cell* **19**, 1251–1264. doi: [10.1105/tpc.106.048355](https://doi.org/10.1105/tpc.106.048355).
- Shutt TE, McBride HM.** 2013. Staying cool in difficult times: mitochondrial dynamics, quality control and the stress response. *Biochimica et Biophysica Acta* **1833**, 417–424. doi: [10.1016/j.bbamcr.2012.05.024](https://doi.org/10.1016/j.bbamcr.2012.05.024).
- Spillane M, Ketschek A, Merianda TT, Twiss JL, Gallo G.** 2013. Mitochondria coordinate sites of axon branching through localized intraxon protein synthesis. *Cell Reports* **5**, 1564–1575. doi: [10.1016/j.celrep.2013.11.022](https://doi.org/10.1016/j.celrep.2013.11.022).
- Takanashi H, Arimura SI, Sakamoto W, Tsutsumi N.** 2006. Different amounts of DNA in each mitochondrion in rice root. *Genes and Genetic Systems* **81**, 215–218. doi: [10.1266/ggs.81.215](https://doi.org/10.1266/ggs.81.215).
- Tinevez JY, Perry N, Schindelin J, Hoopes GM, Reynolds GD, Laplantine E, Bednarek SY, Shorte SL, Eliceiri KW.** 2017. TrackMate: an open and extensible platform for single-particle tracking. *Methods* **115**, 80–90. doi: [10.1016/j.ymeth.2016.09.016](https://doi.org/10.1016/j.ymeth.2016.09.016).
- Twig G, Elorza A, Molina AJA, et al.** 2008. Fission and selective fusion govern mitochondrial segregation and elimination by autophagy. *The EMBO Journal* **27**, 433–446. doi: [10.1038/sj.emboj.7601963](https://doi.org/10.1038/sj.emboj.7601963).
- Virdi KS, Laurie JD, Xu YZ, et al.** 2015. Arabidopsis MSH1 mutation alters the epigenome and produces heritable changes in plant growth. *Nature Communications* **6**, 6386. doi: [10.1038/ncomms7386](https://doi.org/10.1038/ncomms7386).
- Virdi KS, Wamboldt Y, Kundariya H, et al.** 2016. MSH1 is a plant organellar DNA binding and thylakoid protein under precise spatial regulation to alter development. *Molecular Plant* **1**, 245–260. doi: [10.1016/j.molp.2015.10.011](https://doi.org/10.1016/j.molp.2015.10.011).
- Whelan J, Murcha MW.** 2015. *Plant mitochondria: methods and protocols*. New York: Springer. doi: [10.1007/978-1-4939-2639-8](https://doi.org/10.1007/978-1-4939-2639-8).
- Woloszynska M.** 2010. Heteroplasmy and stoichiometric complexity of plant mitochondrial genomes—though this be madness, yet there's method in't. *Journal of Experimental Botany* **61**, 657–671. doi: [10.1093/jxb/erp361](https://doi.org/10.1093/jxb/erp361).
- Wu Z, Waneka G, Broz AK, King CR, Sloan DB.** 2020. MSH1 is required for maintenance of the low mutation rates in plant mitochondrial and plastid genomes. *Proceedings of the National Academy of Sciences, USA* **117**, 16448–16455. doi: [10.1073/pnas.2001998117](https://doi.org/10.1073/pnas.2001998117).
- Xu Y-Z, Arrieta-Montiel MP, Virdi KS, et al.** 2011. MutS HOMOLOG1 is a nucleoid protein that alters mitochondrial and plastid properties and plant response to high light. *The Plant Cell* **23**, 3428–3441. doi: [10.1105/tpc.111.089136](https://doi.org/10.1105/tpc.111.089136).
- Xu YZ, de la Rosa Santamaria R, Virdi KS, et al.** 2012. The chloroplast triggers developmental reprogramming when MutS HOMOLOG1 is suppressed in plants. *Plant Physiology* **159**, 710–720. doi: [10.1104/pp.112.196055](https://doi.org/10.1104/pp.112.196055).
- Yu SB, Pekkurnaz G.** 2018. Mechanisms orchestrating mitochondrial dynamics for energy homeostasis. *Journal of Molecular Biology* **430**, 3922–3941. doi: [10.1016/j.jmb.2018.07.027](https://doi.org/10.1016/j.jmb.2018.07.027).
- Yu Y, Lee HC, Chen KC, Suhan J, Qiu M, Ba Q, Yang G.** 2016. Inner membrane fusion mediates spatial distribution of axonal mitochondria. *Scientific Reports* **6**, 18981. doi: [10.1038/srep18981](https://doi.org/10.1038/srep18981).
- Zheng M, Beck M, Müller J, et al.** 2009. Actin turnover is required for myosin-dependent mitochondrial movements in Arabidopsis root hairs. *PLoS One* **4**, e5961. doi: [10.1371/journal.pone.0005961](https://doi.org/10.1371/journal.pone.0005961).